

## Search for exotic states with $c\bar{c}s\bar{c}$ content at Belle

---

Dmytro Meleshko (*on behalf of Belle collaboration*)

05.03.2024

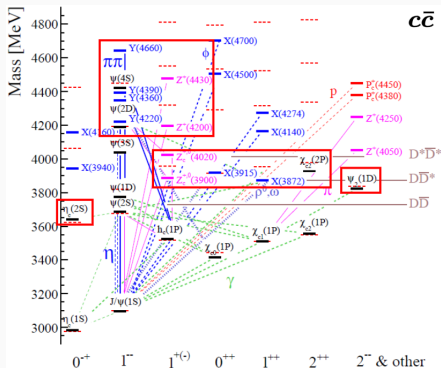
Justus-Liebig-Universität, Giessen, Germany



# Introduction

## Impressive legacy

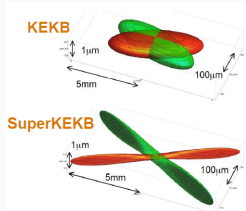
- Many exotic states observed in the past decade are hard to fit these spectra.
- Below  $D\bar{D}/B\bar{B}$  thresholds  $c\bar{c}$  and  $b\bar{b}$  match potential models;



## Life outside $\Upsilon(4S)$ :

- Exotic XYZ states have been observed in different production mechanisms:
  - $B$ -decays ( $0^+$ ,  $1^+$ , ...);
  - ISR ( $1^-$ );
  - $\gamma\gamma$  collisions ( $0^+$ ,  $2^+$ );
- $X(3872)$  and  $T_{cc}^+$  have been observed in  $pp$  inclusive production at LHC. In  $e^+e^-$  collisions this would correspond to continuum production;
- 10% of data taking at Belle is 60 MeV below  $\Upsilon(4S)$
- On-resonance data also contains continuum events (can be separated from  $B$ -decays by event shape);

# From Belle to Belle II: experiment overview

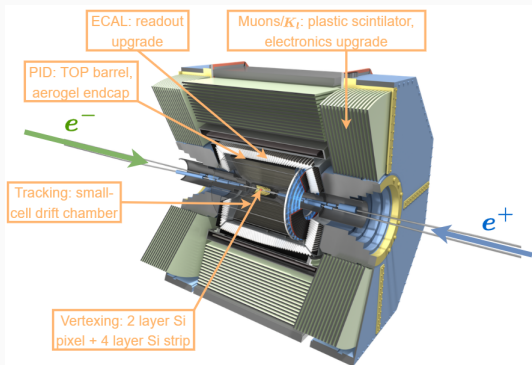


## SuperKEKB:

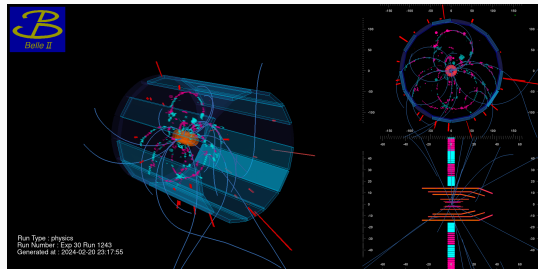
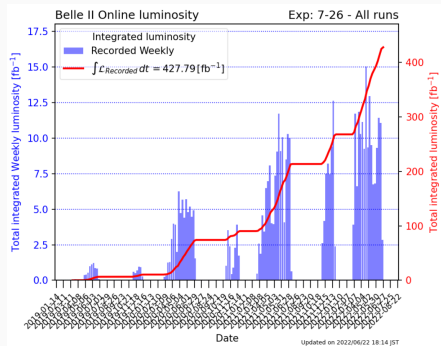
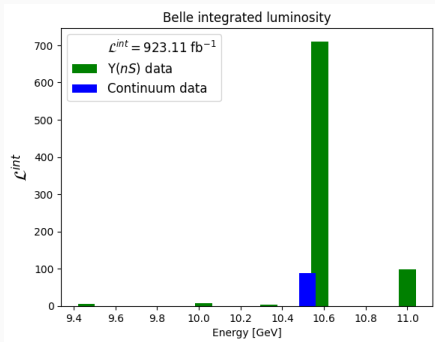
- Asymmetric  $e^+e^-$  collider at KEK (Tsukuba, Japan);
- Energy adjustment: 3.5/8.0 GeV (Belle)  $\rightarrow$  7.0/4.0 GeV (Belle II);
- "Nano-beams"  $\times$  current increase ( $\times 2$ ) =  $\times 30$  inst. luminosity increase;

## Belle II detector upgrade:

- Higher background:
  - Radiation damage;
  - Detector readout;
- Higher event rate ( $\sim 30$  kHz):
  - Trigger, DAQ, computing;
- Boost change:
  - Vertexing improvement;



# What data samples are available today?



20.02.2024 21:12 JST  
First recorded collisions of Run 2

# Introduction

Invariant mass system	Decay from:	Range [GeV/c <sup>2</sup> ]
$D_s^- D_s^+$	$B_s^0$	[3.936 - 5.298]
$D_s^- D_s^+ \pi^0$	$B_s^0$	[4.071 - 5.433]
$D_s^- D_s^{*+}$	$B_s^0$	[4.080 - 5.433]
$D_s^- D_{s0}^*(2317)^+$	$B_s^0$	[4.285 - 5.433]
$J/\psi \phi$	$B^0$	[4.117 - 4.783]
$J/\psi \phi$	$B^\pm$	[4.117 - 4.783]
$J/\psi \phi$	continuum	all range
$D_s^- D_{s0}^*(2317)^+$ , $D_s^- D_{s1}(2460)^+$ , $D_s^- D_s^+ \pi^0, D_s^- D_s^{*+}$	continuum	all range

$$\left. \begin{array}{l}
 B_s^0 \rightarrow D_s^{(*)+} D_s^{(*)-} \pi^0 \\
 \\
 \text{PhD thesis of A. Thampi} \\
 B^{0,\pm} \rightarrow J/\psi \phi K^{0,\pm} \\
 \\
 e^+ e^- \rightarrow J/\psi \phi + \text{anything} \\
 \\
 e^+ e^- \rightarrow D_s^{(*)+} D_s^{(*)-} + \text{anything}
 \end{array} \right\}$$

X(4274)

X(4685)

X(4630)

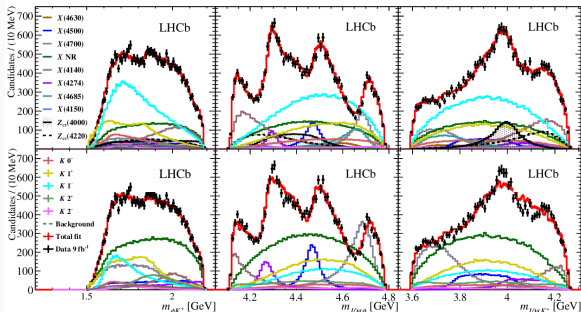
X(4500)

X(4700)

LHCb results:

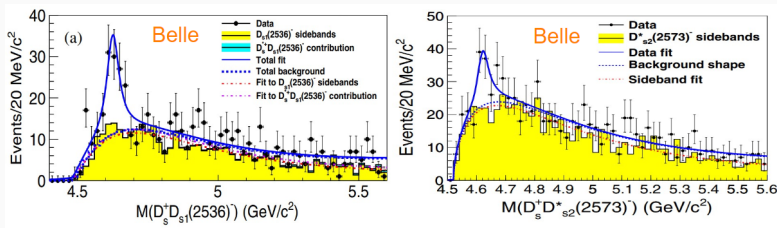
- 9 fb<sup>-1</sup> of data
- 7 neutral X states
- 3 charged Z states

Phys. Rev. Lett. 127, 082001



- A Belle study reported observation of structures with the masses of  $(4625.9^{+6.2}_{-6.0} \pm 0.4)$  MeV and  $(4619.8^{+8.9}_{-8.0} \pm 2.3)$  MeV in the cross-section measurements of  $e^+e^- \rightarrow D_s^+ D_{s1}(2536)^-$  and  $e^+e^- \rightarrow D_s^+ D_{s2}^*(2573)^-$  respectively

Phys. Rev. D 100, no.11, 111103 (2019)    Phys. Rev. D 101, no.9, 091101 (2020)



# Study of $e^+e^- \rightarrow D_s^+ D_{sJ}^- A + \text{c.c.}$ at Belle

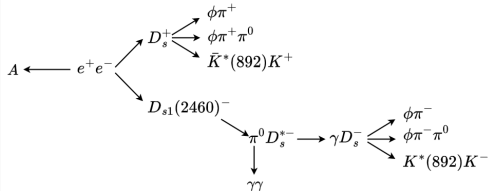
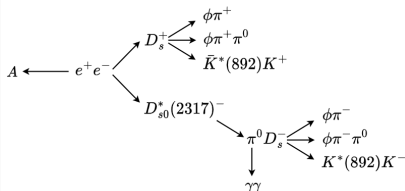
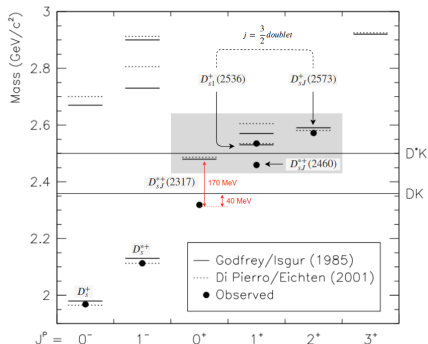
First  $e^+e^- \rightarrow D_s \pi^0 X$  process studies:

- BaBar: 1267 yield on  $91 \text{ fb}^{-1}$
- Belle: 761 yield on  $87 \text{ fb}^{-1}$

Extrapolation from the old analysis with  $D_s^*(2317)$  only, but to the whole data set:

- Belle @ $\Upsilon(4S)$ : 6226 **Only  $D_s^*(2317)$ !**

With one extra  $D_s$  (e.g. +3 charged tracks), efficiency is expected to drop ( $< 1\%$ ). Around 100 events are expected on full Belle dataset.



# Study of $e^+e^- \rightarrow D_s^+ D_{sJ}^- A + \text{c.c.}$ at Belle

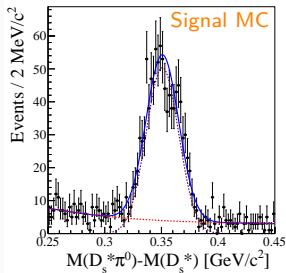
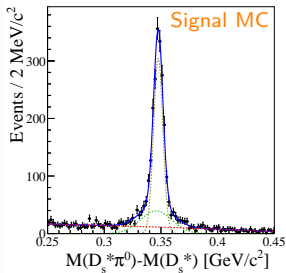
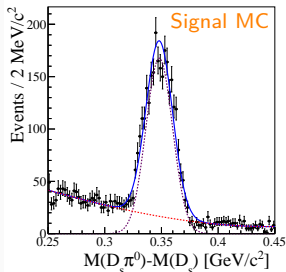
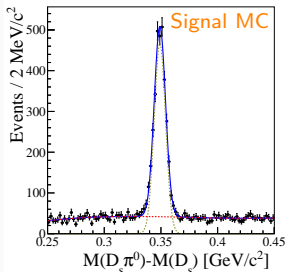
The following peaking contributions are expected

$D_{sJ}(2317)^+$  invariant mass region:

- True  $D_{sJ}(2317)^+$  peak  
 $\sigma = (4.76 \pm 0.8) \text{ MeV}$
- $D_{sJ}(2460)^+$  reflection peak  
 $\sigma = (11.8 \pm 0.3) \text{ MeV}$

$D_{sJ}(2460)^+$  invariant mass region:

- True  $D_{sJ}(2460)^+$  peak  
 $\sigma = (5.07 \pm 0.13) \text{ MeV}$
- $D_{sJ}(2317)^+$  reflection peak  
 $\sigma = (14.6 \pm 0.7) \text{ MeV}$
- $D_{sJ}(2460)^+$  "broken signal"  
 $\sigma = (16.9 \pm 1.8) \text{ MeV}$





# Study of $e^+e^- \rightarrow D_s^+ D_s^- A + \text{c.c.}$ at Belle

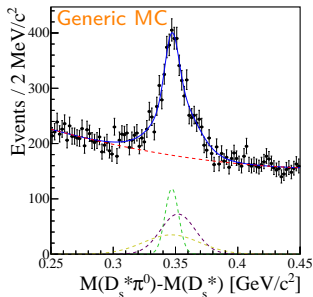
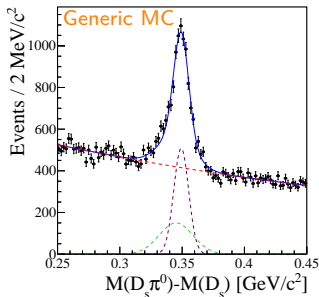
$$\Delta M(D_s \pi^0) = N_1 G(\mu_1, \sigma_1) + f^{\text{down}} N_2 G(\mu^{\text{down}}, \sigma^{\text{down}}) \quad (1)$$

$$\Delta M(D_s^* \pi^0) = N_2 G(\mu_2, \sigma_2) + f^{\text{up}} N_1 G(\mu^{\text{up}}, \sigma^{\text{up}}) + f^{\text{broken}} N_2 G(\mu^{\text{broken}}, \sigma^{\text{broken}})$$

ref:  $N = 3,843 \pm 67$ ,  $\mu = 348.9 \pm 0.1$ ,  $\sigma = 6.20 \pm 0.10$

ref:  $N = 835 \pm 31$ ,  $\mu = 347.1 \pm 0.2$ ,  $\sigma = 5.80 \pm 0.20$

Topology type	$\mu$ , [MeV]	$\sigma$ , [MeV]	N
True $D_{s0}^*$ (2317) signal	$349.3 \pm 0.2$	$5.97 \pm 0.25$	$3,797 \pm 137$
Feed-down background	345.1 (fixed)	13.5 (fixed)	$0.3297 \cdot N_2$
True $D_{s1}$ (2460) signal	$347.1 \pm 0.5$	$5.46 \pm 0.60$	$811 \pm 155$
Feed-up background	352.0 (fixed)	13.9 (fixed)	$3.042 \cdot N_1$
$D_{s1}$ (2460)	346.7 (fixed)	22.7 (fixed)	$1.189 \cdot N_2$



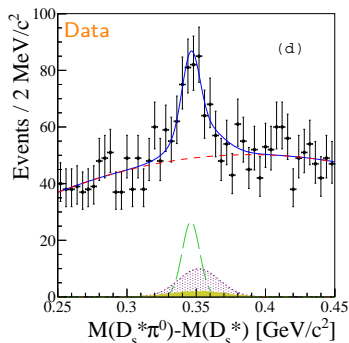
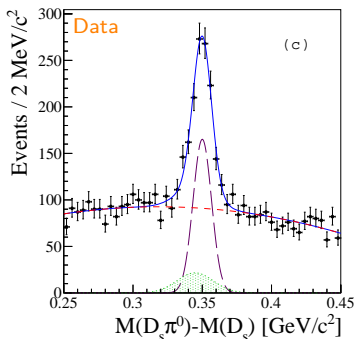
# Study of $e^+e^- \rightarrow D_s^+ D_{sJ}^- A + \text{c.c.}$ at Belle

Cut-based selection  $\rightarrow$  MVA selection

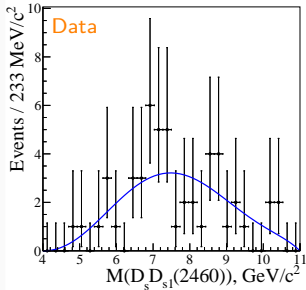
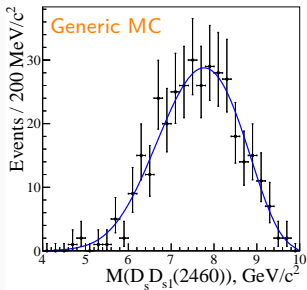
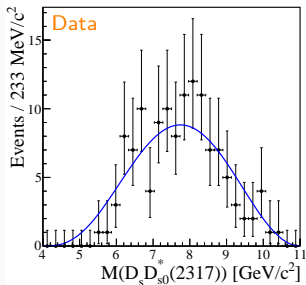
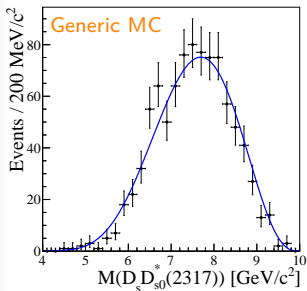
Topology type	$\mu$ , [MeV]	$\sigma$ , [MeV]	N
True $D_{s0}^*$ (2317) signal	$349.6 \pm 0.5$	$7.16 \pm 0.59$	$792 \pm 62$
Feed-down background	344.0 (fixed)	13.4 (fixed)	$0.170 \cdot N_2$
True $D_{s1}$ (2460) signal	$347.3 \pm 1.8$	$6.98 \pm 1.72$	$137 \pm 36$
Feed-up background	349.6 (fixed)	14.6 (fixed)	$2.097 \cdot N_1$
$D_{s1}$ (2460) broken signal	345.5 (fixed)	17.0 (fixed)	$0.231 \cdot N_2$

Cuts:  $N(D_{s0}^*(2317)) = 370 \pm 45$

$N(D_{s1}(2460)) = 68 \pm 22$



# Study of $e^+e^- \rightarrow D_s^+ D_{sJ}^- A + \text{c.c.}$ at Belle



# Study of $e^+e^- \rightarrow D_s^+ D_{sJ}^- A + \text{c.c.}$ at Belle

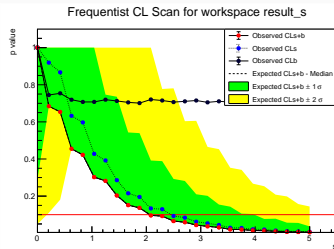
$$\frac{Br(D_{s1}(2460) \rightarrow D_s^* \pi^0)}{Br(D_{s0}^*(2317) \rightarrow D_s \pi^0)} \times \frac{\sigma(D_{s1}(2460), \text{MVA})}{\sigma(D_{s0}^*(2317), \text{MVA})} = 0.26 \pm 0.07(\text{stat}) \pm 0.03(\text{syst})$$

\*The value earlier measured by Belle is  $0.29 \pm 0.06 \pm 0.03$

\*\*The value predicted by theory is 3

$$\sigma^{UL} = \frac{N^{UL} \times |1 - \Pi|^2}{\mathcal{L} \times \sum_{ij} \epsilon_{ij}^* \mathcal{B}_i \mathcal{B}_j \times (1 + \delta)_{ISR}}$$

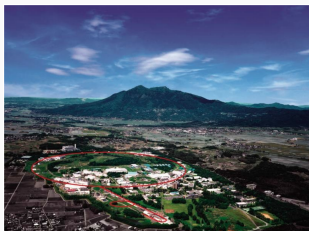
Resonances	$J^P$	$M$ [MeV]	$\Gamma$ [MeV]	Significance
$X(4274)$	$1^+$	$4295 \pm 4_{-6}^{+4}$	$53 \pm 5 \pm 5$	18 (18)
$X(4685)$	$1^+$	$4684 \pm 7_{-16}^{+13}$	$126 \pm 15_{-41}^{+37}$	15 (15)
$X(4630)$	$1^-$	$4626 \pm 16_{-110}^{+18}$	$174 \pm 27_{-73}^{+134}$	5.5 (5.7)
$X(4500)$	$0^+$	$4474 \pm 3 \pm 3$	$77 \pm 6_{-8}^{+10}$	20 (20)
$X(4700)$	$0^+$	$4694 \pm 4_{-3}^{+16}$	$87 \pm 8_{-6}^{+16}$	17 (18)



Decay chain	Total error [%]	Estimated $N_{90}^{UL}$	$\sigma^{UL} \times \mathcal{B}(X \rightarrow D_s D_{sJ}^*)$ [fb]
$e^+e^- \rightarrow X(4274)A$	13.3	2.45	122.5
$e^+e^- \rightarrow X(4685)A$	14.1	2.04	101.8
$e^+e^- \rightarrow X(4630)A$	18.3	2.05	228.1
$e^+e^- \rightarrow X(4500)A$	18.0	2.34	260.1
$e^+e^- \rightarrow X(4700)A$	18.7	2.18	241.8

# Summary

- The process was studied on signal MC, generic MC and data;
- Cut-based and MVA selections were optimized;
- Reconstruction efficiencies are 0.44% and 0.63% for  $D_s D_{s0}^*(2317)$  and  $D_s D_{s1}(2460)$  decay channels with MVA selections, respectively;
- **A precise mass resolution measurement:**
  - $\sigma(D_{s0}^*(2317)) = 7.16 \pm 0.59 \text{ MeV}/c^2$ ;
  - $\sigma(D_{s1}(2460)) = 6.98 \pm 1.72 \text{ MeV}/c^2$ ;
- **A precise  $D_{sJ}$  mass splitting measurement:**
  - $\Delta M(D_s^*(2317)) = 349.6 \pm 0.6 \text{ MeV}/c^2$  (PDG:  $349.4 \pm 0.6 \text{ MeV}/c^2$ );
  - $\Delta M(D_{s1}(2460)) = 347.2 \pm 1.9 \text{ MeV}/c^2$  (PDG:  $347.3 \pm 0.7$  or  $349.1 \pm 0.6 \text{ MeV}/c^2$ );
- Systematic uncertainties evaluated.
- **The estimated ratio of branching fractions is consistent with earlier Belle study.**
- **$D_s D_{sJ}$  invariant mass distributions on data appeared to be PHSP-distributed.**
- **Preliminary cross-section UL for the accessible  $X$  states are evaluated.**



## Backup

---

# Signal MC. Optimized selection and BCS implementation.

In addition to the selection summarized on the right, the BCS selection was applied in the latest iteration of a study.

Selection optimization study has been conducted.

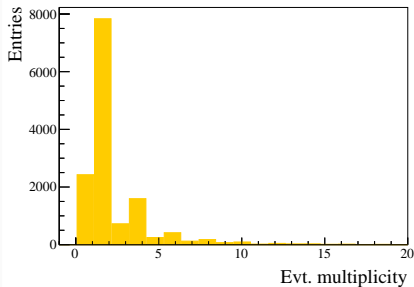


**Figure 1:** Signal MC. Event multiplicity before BCS application.

Particle	Selection criterion
Tracks	$dr < 0.5 \text{ cm}$
	$dz < 3 \text{ cm}$
	$P_{K_1}(K/\pi) > 0.5$
	$P_{K_2}(K/\pi) > 0.2$
$\pi^0$	$P_{\pi}(K/\pi) < 0.9$
	$E(\gamma) > 100 \text{ MeV}$
	$p(\gamma\gamma) > 150 \text{ MeV}/c$
	$\chi^2(\gamma\gamma) < 200$
$\phi$	$122 < M(\gamma\gamma) < 148 \text{ MeV}/c^2$
	$P_{\chi^2}(\gamma\gamma) > 1\%$
	$1.010 < M(KK) < 1.030 \text{ GeV}/c^2$
$K^*(892)$	$P_{\chi^2}(KK) > 0.1\%$
	$842 < M(K\pi) < 942 \text{ MeV}/c^2$
$D_s$	$P_{\chi^2}(K\pi) > 0.1\%$
	$1.9585 < M(D_s) < 1.9785 \text{ GeV}/c^2$
$D_{s0}^*(2317)$	$P_{\chi^2}(D_s) > 0.1\%$
	$p^*(D_s\pi^0) > 2.79 \text{ GeV}/c$
Other	$P_{\chi^2}(D_s\pi^0) > 0.1\%$
	$ \cos\theta_H  > 0.42$

**Table 1:** The summarized selection for  $D_{s1}(2460)$  reconstruction.

\*  $\gamma_*$  denotes the photon combined with  $D_s$  to create  $D_s^*$  candidate decaying into  $D_s\gamma$ .

# Signal MC. $D_s D_{s0}^*(2317)$ system study (threshold case).

$$\epsilon = 0.22 \pm 0.02\%$$

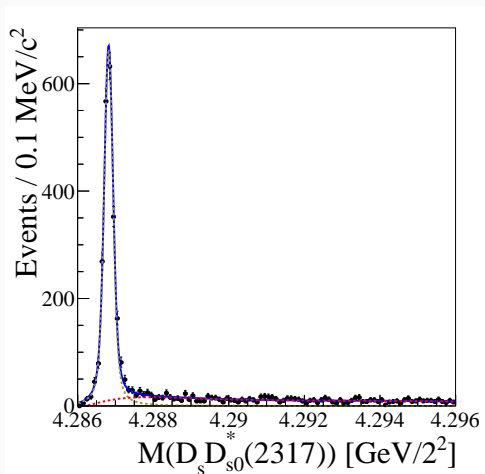


**Figure 2:** The  $D_s D_{s0}^*(2317)$  invariant mass distribution in threshold case. The signal contribution is fitted by Voigt function, non-resonant background as approximated by the Threshold function.



# MVA methods comparison

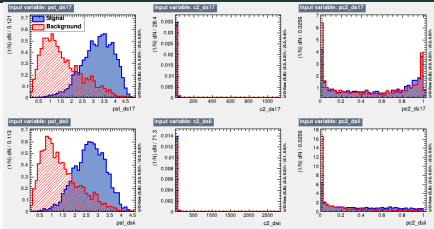


Figure 3: MVA input variables for signal (blue) and background (red) events.

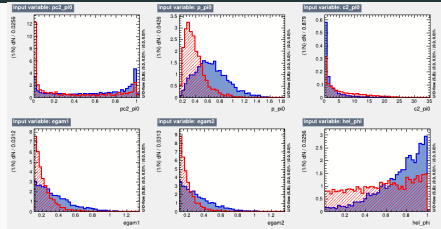


Figure 4: MVA input variables for signal (blue) and background (red) events.

- Pre-selection is applied.
- Performances of MLP, BDT, Fisher and DNN methods are compared → **MLP is chosen**
- Set of input variables is optimized with respect to correlation matrix → **redundant variables eliminated.**

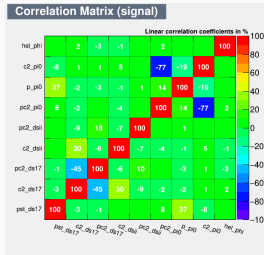


Figure 5: Input parameters Correlation Matrix for signal events.

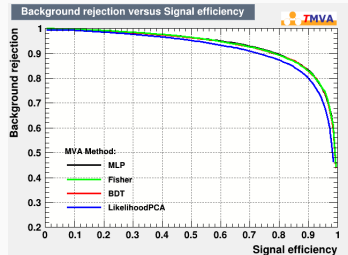


Figure 6: ROC curve.

# MLP application

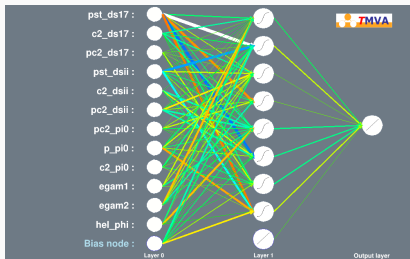


Figure 7: MLP architecture.

## MLP Convergence Test

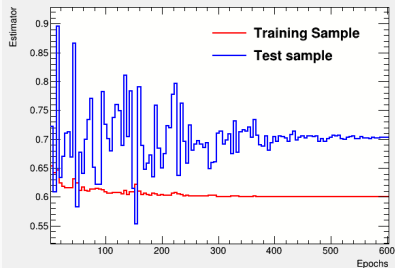


Figure 9: MLP convergence test.

## TMVA response for classifier: MLP

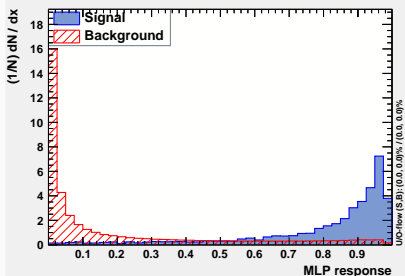


Figure 8: MLP response for classifier on training sample.

## Cut efficiencies and optimal cut value

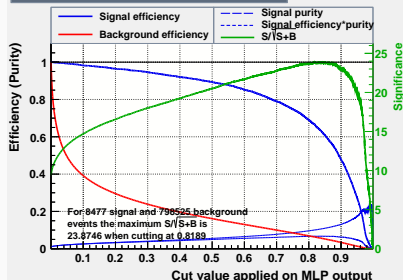


Figure 10: FoM dependence on classifier cut value.

## Systematic uncertainties

Systematic Contribution	$D_s D_{s0}^*(2317)$ %	$D_s D_{s1}(2460)$ %
Charged tracks identification	3.21	3.21
Track reconstruction	2.10	2.10
MC statistics	1.82	2.42
Integrated luminosity	1.40	1.40
$\pi^0$ reconstruction	2.00	2.00
$\gamma$ reconstruction	-	2.30
Secondary BF	5.83	5.62
Background fit PDF order	1.03	1.23
Mass cuts on secondary particles	5.58	7.80
TOTAL	9.50	11.22

# Asymptotic method

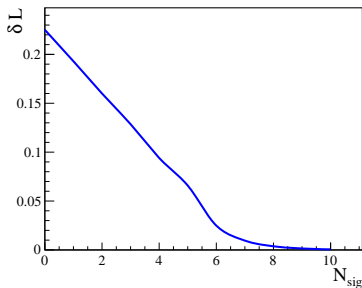
Equation to solve:

$$\frac{\int_0^{N^{90\%}} \mathcal{L}(x) dx}{\int_0^{+\infty} \mathcal{L}(x) dx} = 0.9 \quad (2)$$

$N^{90\%}$  - wanted UL on the number of signal events.

Target dependency to study:

$$\Delta L = e^{\mathcal{L}(N_{sig}) - \mathcal{L}_0} \quad (3)$$



Consideration of the systematic uncertainties:

$$\Delta(\Delta L) = \frac{\Delta \mathcal{L}_j \cdot \mathcal{L}_j}{\sqrt{2\pi \varepsilon_{syst} N_j^{sig}}} \cdot e^{-\frac{1}{2} \left( \frac{\Delta N_j^{sig}}{\varepsilon_{syst} N_j^{sig}} \right)^2} \quad (4)$$

Cross-section UL calculation:

$$\sigma^{90\%} = \frac{N^{90\%}}{\varepsilon^{tot} \cdot \mathcal{L}^{int}} \quad (5)$$

## Likelihood ratio:

$$\lambda(\mu) = \frac{\mathcal{L}(\mu, \hat{\theta} | n_1, \dots, n_{N_b})}{\mathcal{L}(\mu, \hat{\theta} | n_1, \dots, n_{N_b})}, \quad (6)$$

where  $(\mu, \hat{\theta})$  are the parameters that maximize the likelihood for the set of observations  $n_1, \dots, n_{N_b}$ ; and  $\hat{\theta}$  maximizes the likelihood for a given value of  $\mu$ .

## Test statistics $q_\mu$ :

$$q_\mu = \begin{cases} -2\ln\lambda(\mu) & \text{if } \mu > \hat{\mu}, \\ 0 & \text{otherwise} \end{cases} \quad (7)$$

The level of agreement between the data and the hypothesized value of  $\mu$  is quantified with the  $p$ -value:

$$p_{s+b} = P(q_\mu > q_{\mu, \text{obs}} | \mu) = \int_{q_{\mu, \text{obs}}}^{\infty} p(q_\mu | \mu) dq_\mu, \quad (8)$$

where  $> q_{\mu, \text{obs}}$  is the observed value of  $q_\mu$ , and  $p(q_\mu | \mu)$  denotes the probability density function of  $q_\mu$  under the assumption of a signal strength of  $\mu$ .

**UL on  $\mu$  at 90% CL is the largest value of  $\mu$  such as  $p_{s+b}$  stays above 0.1**

